Materials Today Bio 21 (2023) 100693

Contents lists available at ScienceDirect

Materials Today Bio

journal homepage: www.journals.elsevier.com/materials-today-bio

Fullerene [60] encapsulated water-soluble supramolecular cage for prevention of oxidative stress-induced myocardial injury

Guanzhao Zhang [a,1], Hui Fang [b,c,1], Shuting Chang [e], Renzeng Chen [b], Lanlan Li [f], Danbo Wang [b], Yamei Liu [d], Ruyi Sun [c,**], Yingjie Zhao [b,*], Bo Li [a,***]

[a] Department of Cardiology, Binzhou Medical University, Zibo Central Hospital, NO.10, South Shanghai Road, Zibo, 255000, China
[b] College of Polymer Science and Engineering, Qingdao University of Science and Technology, Qingdao, 266042, China
[c] School of Chemistry and Molecular Engineering, East China Normal University, 500 Dongchuan Road, Shanghai, 200241, China
[d] School of Chemistry and Chemical Engineering, Frontiers Science Center for Transformative Molecules, Shanghai Key Laboratory of Electrical Insulation and Thermal Ageing, Shanghai Jiao Tong University, Shanghai 200240, China
[e] Weifang Medical University, NO.7166, Baotong West Street, Weifang, 261053, China
[f] Center of Translational Medicine, Zibo Central Hospital, NO.10, South Shanghai Road, Zibo, 255000, China

ARTICLE INFO

Keywords:
Oxidative stress
Molecular cage
Fullerene
Akt/Nrf2/HO-1 pathway
Myocardial cells

ABSTRACT

A water-soluble cube-like supramolecular cage was constructed by an engagement of six molecules through a hydrophobic effect in the water. The obtained cage could perfectly encapsulate one fullerene C_{60} molecule inside of the cavity and significantly improve the water-solubility of the C_{60} without changing the original structure. The water-soluble complex was further applied to reduce the reactive oxygen species (R.O.S.) in cardiomyocytes (FMC84) through Akt/Nrf2/HO-1 pathway. Furthermore, in the mouse model of myocardial ischemia-reperfusion injury, the application of C_{60} was found to be effective in reducing myocardial injury and improving cardiac function. It also reduced the levels of R.O.S. in myocardial tissue, inhibited myocardial apoptosis, and mitigated myocardial inflammatory responses. The present study provides a new guideline for constructing water-soluble C_{60} and verifies the important role of C_{60} in preventing oxidative stress-related cardiovascular disease injury.

1. Introduction

Acute myocardial infarction (A.M.I.) is the primary cause of mortality associated with cardiovascular disease [1]. Myocardium can experience insufficient oxygen supply due to coronary artery obstruction, leading to myocardial necrosis, fibrosis, and ventricular remodeling, severely affecting heart function [2–4]. Reperfusion therapy remains the primary approach for alleviating A.M.I., as it can relieve myocardial cell hypoxia, improve heart function, reduce infarct size progression, and effectively and promptly reduce mortality rates [5]. During ischemia-reperfusion, there is burst-like production of reactive oxygen species (R.O.S.), when present in excess quantities, may cause myocardial cell death, induce inflammatory reactions, and cause myocardial contractile dysfunction, arrhythmias, and myocardial infarction [6,7]. The production of reactive oxygen species (R.O.S.) is based on continuous oxidative stress. The oxidative stress process has been proven to be involved in the pathogenesis of cardiovascular diseases such as hypertension, aortic aneurysm, hypercholesterolemia atherosclerosis, cardiac ischemia-reperfusion injury, myocardial infarction, heart failure and cardiac arrhythmias [8,9]. Therefore, a good balance between R.O.S. and antioxidants is essential for the normal function of cells [10–13]. Cardiovascular disease-related pro-inflammatory cytokines have a very well-established relationship with R.O.S [14]. The current antioxidant therapy strategies mainly include dietary assistance, gene therapy, free radical scavengers, polyethylene glycol (P.E.G.) binding, and nanomedicine-based technology. However, the effect and application are not satisfactory [15,16]. In view of the limitations of the above methods, it is very important to find an efficient and powerful antioxidant to prevent the occurrence and

Abbreviations: ROS, reactive oxygen species; AMI, acute myocardial infarction; PEG, polyethylene glycol; WB, Western Blot; I/R, ischemia-reperfusion.

* Corresponding author.
** Corresponding author.
*** Corresponding author.
E-mail addresses: rysun@chem.ecnu.edu.cn (R. Sun), yz@qust.edu.cn (Y. Zhao), libosubmit@163.com (B. Li).
[1] These authors contributed equally to this work.

https://doi.org/10.1016/j.mtbio.2023.100693
Received 10 March 2023; Received in revised form 5 June 2023; Accepted 6 June 2023
Available online 17 June 2023

development of the disease.

Fullerenes and their derivatives are called "free radical sponges" due to their highly electron-deficient structure and accessibility to radicals [17–19]. In addition, the antioxidant activity [20], antibacterial activity [21], antiviral activity [22], carrier drug [23] and tumor therapy [24] activity of the fullerenes have been widely accepted in the fields of biology and medicine [25–27]. However, the spherical and hydrophobic surface of fullerenes often results in limited solubility in water. Many efforts have been done to increase the water solubility of C_{60} to expand its usage in biomedical applications [26,28]. Most of the attempts were to modify the chemical structure of $C_{60,}$ for example, by introducing hydrophilic groups into C_{60} [29,30]. The functionalization of the original structure of C_{60} would definitely bring some performance loss, especially the electron-deficient characteristic, for example. The opening of the double bonds in the typical reaction of C_{60} modification would influence the overall conjugation of C_{60}. To keep the original structure of C_{60} and significantly improve the water solubility would be an ideal goal.

The supramolecular self-assembly may provide an ideal solution. As we know, the self-assembly of amphiphile molecules has been widely used to construct various nanostructures containing channels and cavities in water [31–33]. The best-known examples are micelles and vesicles which could be easily triggered by conventional amphiphiles with a hydrophilic head and hydrophobic tail in aqueous media [34–36]. However, the precise control of the cavities is still hard to realize due to the random self-assembly process. The cavities or channels made by nature have played a central role in biochemical processes [37]. For example, selective encapsulation of substrates within the confined cavities of enzymes, immunological antigen-antibody association, cellular recognition, and so on are all important biological processes. To mimic these nano-environments in nature, the artificially prepared, well-defined self-assembled structures with specific cavities could provide a suitable confined environment that allows guests to be selectively encapsulated and released, with consequent control over their reactivities. The construction of such self-assembled nanostructures in water shows great potential in biological and medical domains [38,39]. Molecular cages are perfect model systems for studying the concept of the confined environment in the biological system [40,41]. Much effort has been made to control the precise structures of the molecular cages. A large number of molecular cages with different sizes, shapes, and functions have been prepared [42–44]. They have shown multiple functionalities based on their confined inner environment like enzymes do in biological systems [45,46]. However, most synthetic organic covalent cages are neutral with poor solubility in water. And the large cage formation in water has mostly been limited to metal-organic cages based on the non-covalent metal coordination processes [38,47]. Self-assembly of small water-soluble molecules in complex architectures is becoming a promising strategy for the construction of novel cage-like structures in water.

This work intends to prepare water-soluble molecular cages with a well-defined structure through the self-assembly of small water-soluble molecules. The size of the molecular cage is regulated by molecular design so that it can selectively complex functional molecules such as fullerenes. The water solubility of the cage/fullerene complex may be achieved without destroying the structure of fullerene, which greatly retains the molecular integrity and biomedical activities [48–50]. To be specific, inspired by the traditional burr puzzle game, we designed a hexagram-shaped amphiphile ($\mathbf{M_1}$) with six hydrophilic vinylpyridyl groups attached to a hydrophobic hexaphenyl benzene core (Fig. 1). The hydrophobic effect played a key role in the self-assembly process. The single-crystal X-ray diffraction gave clear evidence of the cube-like structures assembled from six monomers of $\mathbf{M_1}$ in pure water by the hydrophobic effect. In addition, the cage can encapsulate a C_{60} molecule

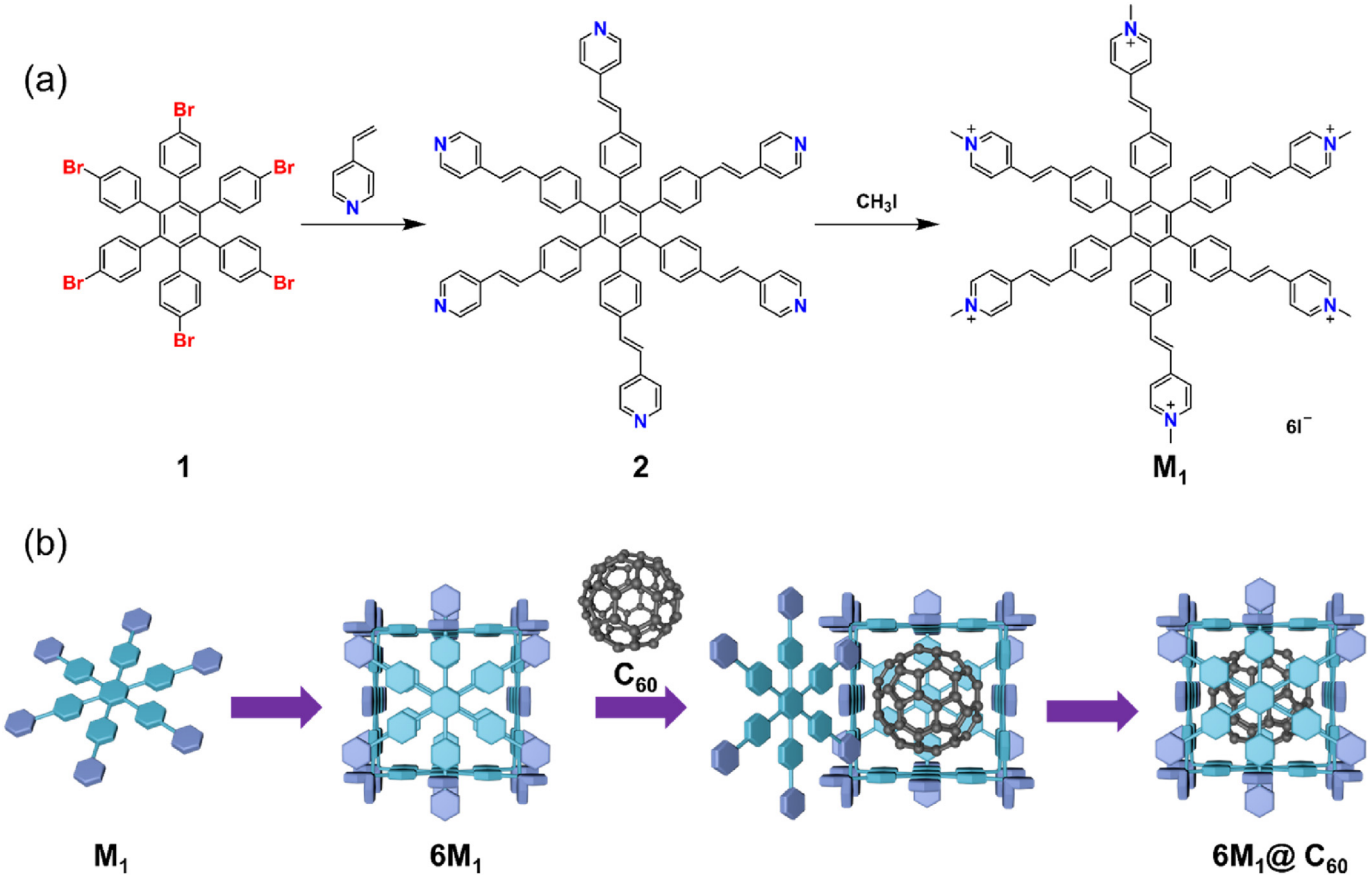

Fig. 1. Synthesis route of $\mathbf{M_1}$ (a) and the schematic representation of self-assembly of $\mathbf{M_1}$ to form the **cage** $\mathbf{6M_1}$ and the complex $\mathbf{6M_1@C_{60}}$ (b).

in the hydrophobic interior space and lead to a significant improvement in the water solubility of C_{60}. The **$6M_1@C_{60}$** complex was further applied to reduce the R.O.S. in the cardiomyocyte. Notably, **$6M_1@C_{60}$** could significantly reduce H_2O_2-induced intracellular R.O.S. levels and further slow down the apoptosis and inflammatory responses with better cell viability in cardiomyocytes (FMC84). In the mouse model of myocardial ischemia-reperfusion injury, the application of **$6M_1@C_{60}$** was found to be effective in reducing myocardial injury and improving cardiac function. It also reduced the levels of R.O.S. in myocardial tissue, inhibited myocardial apoptosis, and mitigated myocardial inflammatory responses. The whole process has been confirmed through Akt/Nrf2/HO-1 pathway. These results are significant for the treatment of oxidative stress-related cardiovascular diseases.

2. Results and discussion

2.1. The synthesis and characterization of the molecular cage

The synthesis of **M_1** is very straightforward. As shown in Fig. 1 and 1–5,6-hexakis (4-bromophenyl)benzene (**1**) is commercially available. Compound **2** was synthesized through Heck reaction between **1** and 4-vinylpyridine. The subsequent methylation reaction led to the target

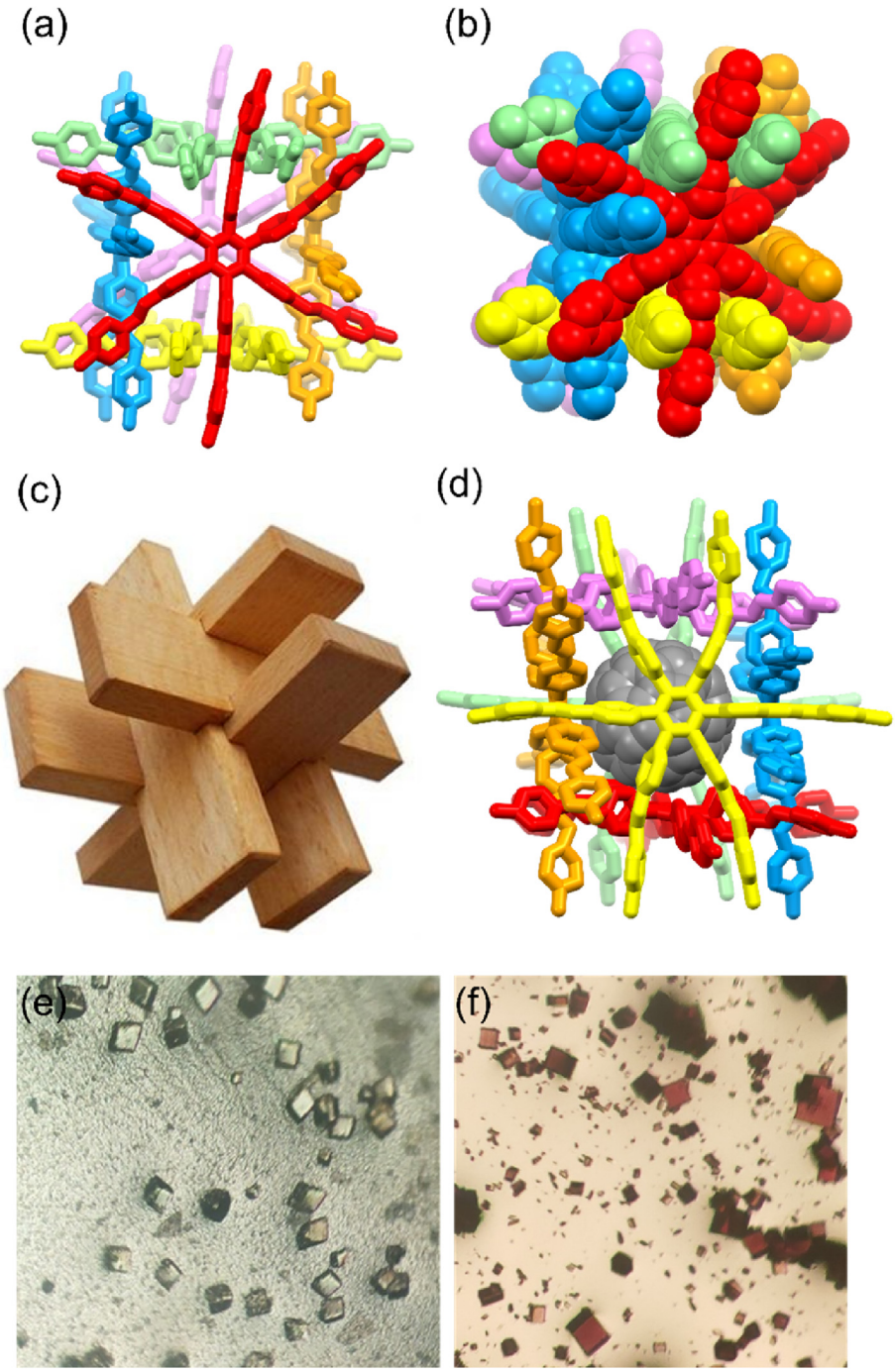

Fig. 2. Single-crystal structure of the cage **$6M_1$** (a) stick style and (b) spacefill style (The hydrogen atoms, H_2O molecules and the iodine ions are omitted due to clarity). (c) A picture of the burr puzzle game box. (d) Optimized structure of the **$6M_1@C_{60}$** complex. (e) Optical microscopy image of **$6M_1$** single crystals. (f) Optical microscopy image of **$6M_1@C_{60}$** single crystals.

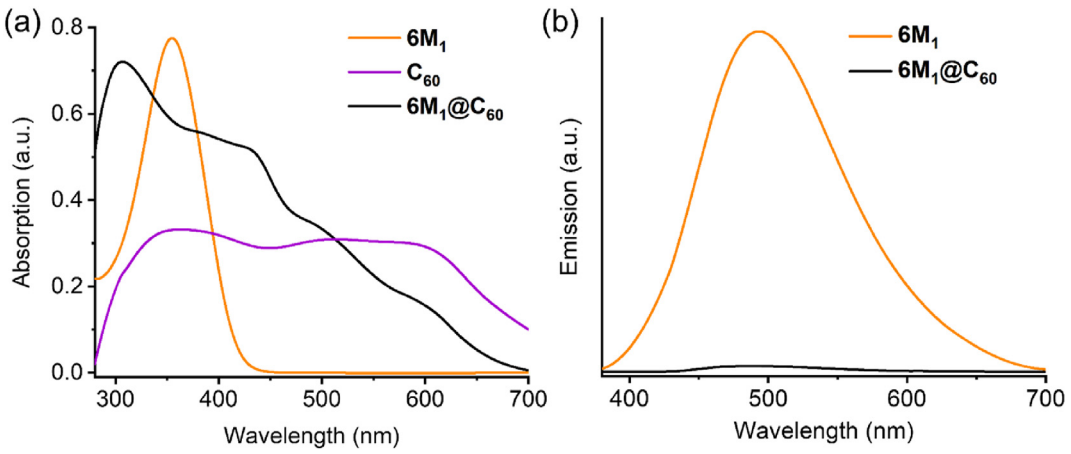

Fig. 3. (a) UV–Vis spectra of **6M$_1$** and the complex **6M$_1$@C$_{60}$** in H_2O at 25 °C (1.6×10^{-5} mol/L) and C_{60} in o-dichlorobenzene at 25 °C (2.6×10^{-6} mol/L). (b) Fluorescent spectra of **6M$_1$** and **6M$_1$@C$_{60}$** (1.6×10^{-5} mol/L) in H_2O at 25 °C.

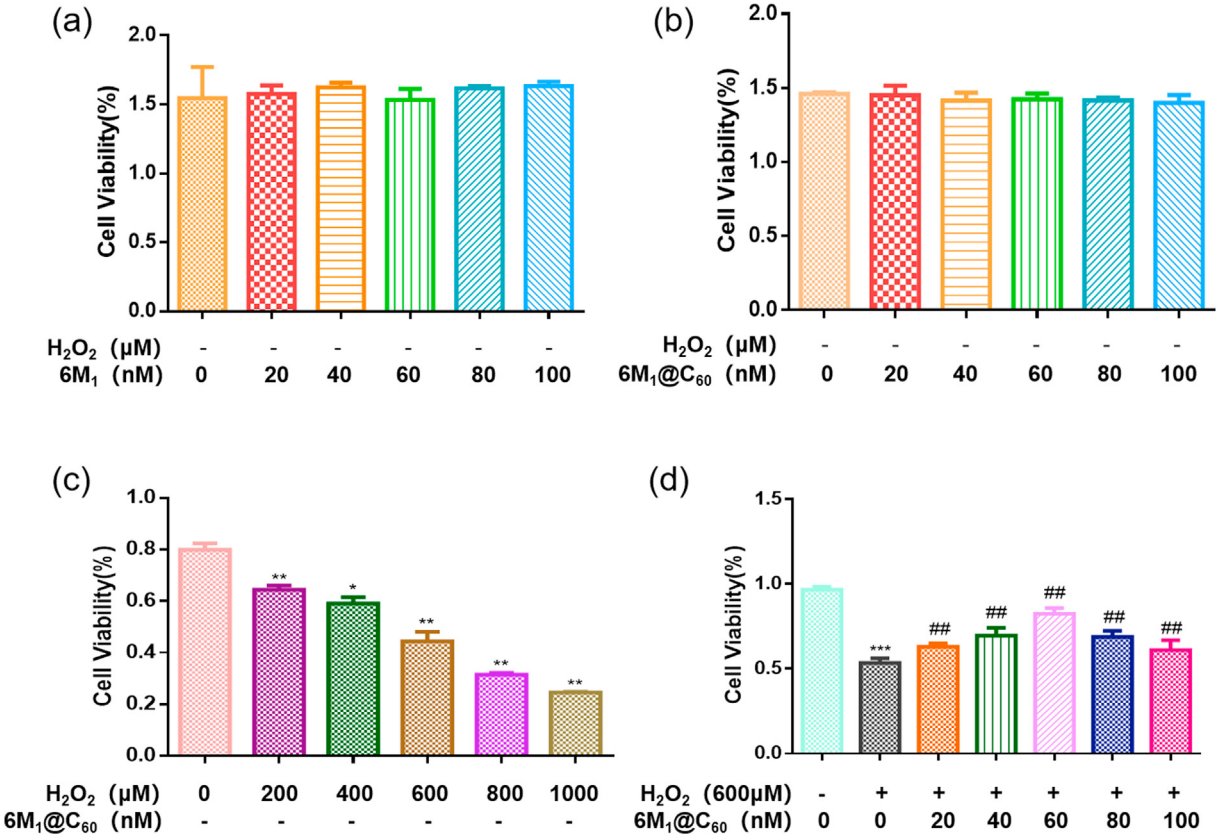

Fig. 4. The effect of H_2O_2 and **6M$_1$@C$_{60}$** on the viability of mouse cardiomyocytes. (a) CCK-8 assay was used to detect the effect of **6M$_1$** (20, 40, 60, 80 and 100 nM) incubation for 6 h on the viability of FMC84 cells. (b) CCK-8 assay was used to detect the effect of **6M$_1$@C$_{60}$** (20, 40, 60, 80 and 100 nM) incubation for 6 h on the viability of FMC84 cells. (c) CCK-8 assay was used to detect the effect of H_2O_2 (200, 400, 600, 800 and 1000 μM) incubation for 6 h on the viability of FMC84 cells. (d) CCK-8 was used to detect the effect of **6M$_1$@C$_{60}$** on the viability of FMC84 cells induced by H_2O_2.(Data are presented as the mean ± S.D.,n = 3, *P < 0.05, **P < 0.01 means significant difference compared from control group , $^{\#}$P < 0.05,$^{\#\#}$p < 0.01 means significant difference compared with H_2O_2 group)

molecule **M$_1$**. The detailed synthesis procedure was presented in the Supplementary Material.

The solubility of the **M$_1$** in water is ~10 mg/mL at 25 °C. However, the ^{1}H NMR spectrum of **M$_1$** in D_2O showed a very complicated spectral pattern (Fig. S1), while that in DMSO-d_6 was very clear and matched well with the structure of **M$_1$** (Fig. S1). This suggests the formation of aggregates in water. To figure out the exact self-assembled structure of **M$_1$** in water, a single crystal of **M$_1$** was obtained through a very slow cooling process of recrystallization in a mixture of water and ethanol. A screw cap vial (2 mL) charged with **M$_1$** (10.0 mg) and H_2O/ethanol (150 μL, 9:1 by vol.) was mounted in a thermo-block which could control precisely the rate of heating or cooling. The vial was heated up to 100 °C within 10 min and maintained 10 min at this temperature to ensure that all the **M$_1$** has completely dissolved. Then, the set-up was slowly cooled down from 100 °C to 25 °C within 1 h to obtain single crystals. The single crystals of **M$_1$** are colorless and exhibit regular cubic shapes (Fig. 2c). Single-crystal X-ray diffraction analysis gave the atomic-resolution structure of **M$_1$**. As shown in Fig. 2a and b, six molecules of **M$_1$** engage with each other and

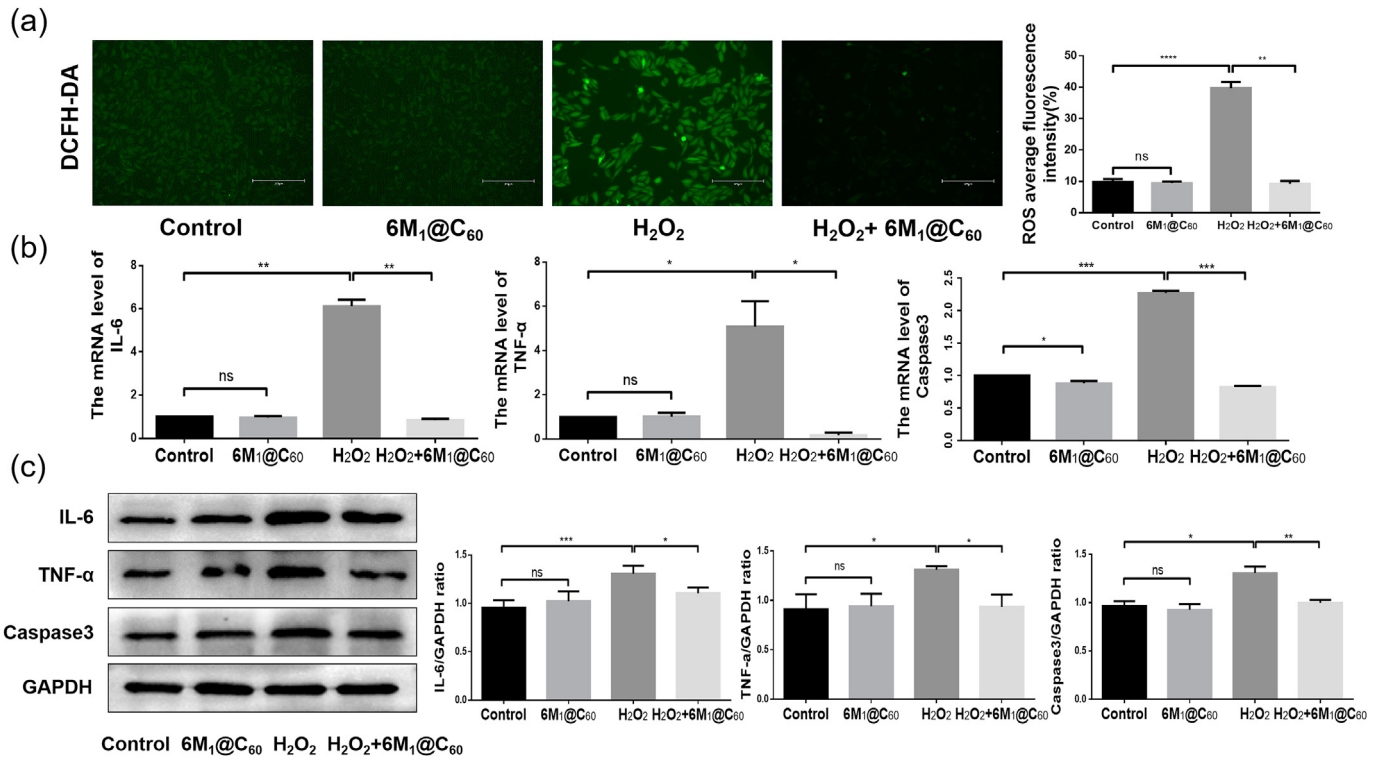

Fig. 5. (a) The fluorescence probe DCFH-DA was used to detect intracellular R.O.S. levels, Bar = 300 μm. (b) The expression of IL-6, TNF-α and Caspase3 in cells was detected by RT-qPCR. (c) The expression of IL-6, TNF-α and Caspase3 in cells was detected by W.B. (Data are presented as the mean ± S.D.,n = 3, *P < 0.05, **P < 0.01, ***P < 0.001, N.S. means not significant).

form a perfect cube. Each **M_1** molecule acts as one of the square faces in the cube, just like the traditional burr puzzle game shown in Fig. 2c. The hydrophilic ends in the arms of **M_1** tend to stay together to create a hydrophilic periphery of the cube. The iodide ions as counter anions stay around the external surface of the cube. A hydrophobic cavity with a diameter of ~1.4 nm was finally constructed. The hydrophobic characteristic and the size of the cage led us to the idea of the encapsulation of hydrophobic C_{60} inside the cage.

2.2. *The nanoencapsulation of C_{60} molecules*

We then try to encapsulate the C_{60} molecule into the obtained cube cage **$6M_1$**. The solution of **M_1** (6 mg) in the mixture of water/ethanol (90 μL, 9:1 by vol) was heated up to 100 °C. A saturated solution of C_{60} in *o*-dichlorobenzene and ethanol (90 μL, 9:1 by vol) was heated up to 100 °C then added to the **M_1** solution. The mixture system was kept at 100 °C for 10 min. Then, the mixture solution was slowly cooled down from 100 °C to 25 °C within 1 h to obtain the co-crystal of **$6M_1@C_{60}$**. The co-crystals were isolated as dark-brown crystals, the color of the complex is distinguished from the crystal of cage **$6M_1$** itself (light yellow) (Fig. 2e and f). Although the crystal looks high-quality from optical microscopy, single-crystal X-ray diffraction analysis failed to give clear structure information of the co-crystal due to the weak signals at high angles. The introduction of the C_{60} to the cage induces some disorder in the crystal. It is understandable because the highly symmetric C_{60} molecules as guests are usually disordered in the crystal cavity [51,52]. However, the UV–Vis absorption spectra of **$6M_1$** and **$6M_1@C_{60}$** show obvious differences. A wide C_{60} absorption peak was observed in the complex, which indicated the presence of C_{60} (Fig. 3a). In the fluorescence spectrum, an obvious fluorescence decrease was also observed when the C_{60} molecule was encapsulated in cage **$6M_1$** (Fig. 3b). All the results above indicated the successful self-assembly of **$6M_1$** and C_{60} in water. Geometry optimization of the established **$6M_1@C_{60}$** models was performed by the Materials Studio Forcite Module, which is an advanced classical molecular mechanics tool and allows for fast and reliable geometry optimization and energy calculations. As shown in Fig. 2d, the cavity of cage **$6M_1$** perfectly matches the size of **C_{60}**.

2.3. *The effect of H_2O_2 and $6M_1@C_{60}$ on the viability of mouse cardiomyocytes*

Taking into consideration the improved water solubility and the radical scavenger activity of the C_{60}, we then tested the effect of **$6M_1@C_{60}$** on the viability of cardiomyocytes (FMC84) in the presence of H_2O_2. When **$6M_1$** or **$6M_1@C_{60}$** were incubated, cell survival was not affected (Fig. 4a and b). This demonstrated that the toxicity of the **M_1** is minimal. While the cell viability was affected by H_2O_2 in a concentration-dependent manner. Stimulation with 600 μM H_2O_2 for 6 h in the following assay resulted in a reduction of 40%–50% in cell viability compared to the control group (Fig. 4c). Under the optimum concentration and time of hydrogen peroxide, different concentrations of **$6M_1@C_{60}$** were added. The results showed that the 60 nM **$6M_1@C_{60}$** could improve H_2O_2-induced myocardial injury significantly (Fig. 4d).

2.4. *Inhibiting H_2O_2-induced cardiomyocyte apoptosis and inflammation*

R.O.S. is a key factor causing apoptosis and inflammatory grading. Activation of apoptotic proteins is the beginning of programmed cell death, accompanied by inflammation. Therefore, scavenging R.O.S. helps to improve apoptosis and inflammatory response [53]. In this experiment, we detected intracellular R.O.S. induced by H_2O_2 and the elimination through the addition of **$6M_1@C_{60}$**. H_2O_2 could significantly increase R.O.S. levels. While the introduction of **$6M_1@C_{60}$** significantly decreased the intracellular R.O.S. level (Fig. 5a). In addition, the effects of H_2O_2 on pro-inflammatory cytokines such as IL-6 and TNF-α were also investigated by RT-qPCR and W.B. The results indicated that H_2O_2 increased the expression of IL-6,TNF-α and Caspase3, whereas **$6M_1@C_{60}$** abolished this change (Fig. 5b and c). Caspase3 is the most critical

apoptotic executor protease during apoptosis. W.B. data showed that H_2O_2 increased caspase3 expression, whereas the treatment with **$6M_1@C_{60}$** inhibited the change (Fig. 5c). Hoechst apoptosis detection kit and flow cytometry also showed that **$6M_1@C_{60}$** improved H_2O_2-induced apoptosis (Fig. 6a and b). The above results show that **$6M_1@C_{60}$** has a protective effect against H_2O_2-induced oxidative stress injury. (Data are presented as the mean ± S.D., n = 3, *P < 0.05, **P < 0.01, ***P < 0.001)

2.5. The *$6M_1@C_{60}$* ameliorated myocardial I/R injury in mouse at an early stage

The free radical theory is an important mechanism in myocardial I/R injury, and the production of R.O.S. not only accelerates the necrosis of myocardial cells but also causes the deterioration of cardiac function. In order to investigate the role of **$6M_1@C_{60}$** in I/R injury, we compared the extent of myocardial injury in various groups using TTC staining after 30 min of ischemia and 2 h of reperfusion. The results showed that the injection of different concentrations of **$6M_1@C_{60}$** could moderately reduce the area of myocardial injury (Fig. 7a). Further analysis of mouse cardiac function was conducted using ultrasound cardiography and HE staining, and the results showed that compared with the sham operation group, the model group (I/R) had significantly increased LVIDd and LVIDs values, decreased LVEF and LVFS values (P < 0.05), and injection of **$6M_1@C_{60}$** could dose-dependently improve mouse cardiac function (Fig. 7b and c). Additionally, HE staining showed that compared with the sham operation group, the I/R group had significant necrotic changes in the muscle fibers, interstitial edema, and mild fibrosis. The focal tissue necrosis and interstitial edema of the **$6M_1@C_{60}$** group were significantly reduced and dose-dependent (Fig. 7d).

2.6. *$6M_1@C_{60}$* can reduce the level of R.O.S., apoptosis and inflammation in myocardial ischemia-reperfusion area

With the progression of reperfusion, the explosive accumulation of R.O.S. damages the cell membrane and exacerbates the necrosis of hypoxic cells, leading to more severe inflammation and further aggravating myocardial damage. To further investigate the ability of **$6M_1@C_{60}$** to scavenge oxygen free radicals, we measured R.O.S. levels in the ischemia-reperfusion area. The results showed that compared with the sham operation group, the I/R group had significantly increased R.O.S. levels, and injection of **$6M_1@C_{60}$** could dose-dependently reduce the R.O.S. levels in the reperfusion area (Fig. 8a); to observe myocardial survival in the reperfusion area, we used Tunel staining to fluorescently label apoptotic myocardium, and the results showed that compared with the sham operation group, the I/R group had massive myocardial necrosis, and injection of **$6M_1@C_{60}$** could dose-dependently reduce myocardial cell apoptosis (Fig. 8b). In addition, immunohistochemistry was used to detect the expression of the inflammatory markers IL-6 and TNF-α in the reperfusion area. The results showed that I/R caused severe inflammation, while injection of **$6M_1@C_{60}$** could dose-dependently alleviate the inflammation in the reperfusion area (Fig. 8c and d).

2.7. Attenuation of inflammatory response and apoptosis by activating Akt pathway and Nrf2/HO-1 pathway

Akt signal transduction pathway is closely related to proliferative diseases such as promoting cell growth and inhibiting cell apoptosis and also plays an important role in regulating diseases related to oxidative stress [54]. We then determined the phosphorylation and total expression levels of Akt, Nrf2 and HO-1 in cells treated with **$6M_1@C_{60}$** by WB. As shown in (Fig. 9a), **$6M_1@C_{60}$** treatment further significantly increased the intracellular expression levels of Akt, Nrf2 and HO-1, indicating that **$6M_1@C_{60}$** may be involved in the regulation of the Akt and Nrf2/HO-1 pathway. In order to verify whether there is a regulatory relationship between the Akt pathway and Nrf2/HO-1 pathway in this study, we selected an Akt inhibitor (MK2206). MK2206 is a highly selective Akt 1/2/3 inhibitor, and pretreatment with MK2206 significantly inhibited the phosphorylation of Akt. With the decrease of p-Akt protein expression, the expressions of Nrf2 and HO-1 proteins were successively decreased,

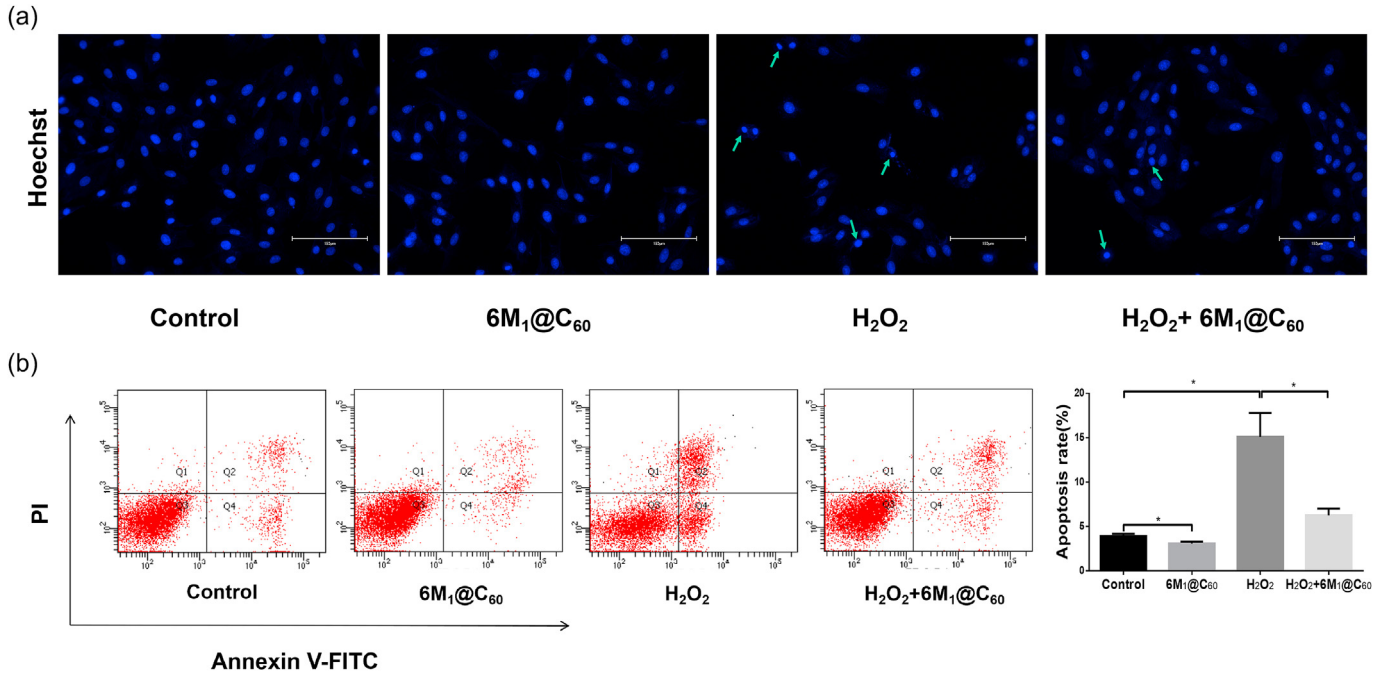

Fig. 6. (a) Apoptotic cells were detected by Hoechst, Bar = 150 μm. (b) Evaluation of apoptosis by flow cytometry. FITC-labeled Annexin V and fluorescent dye PI were used to stain cells. The data were presented as percent apoptotic cells versus total cells. The apoptotic cell percentage was calculated. (Data are presented as the mean ± S.D.,n = 3, *P < 0.05)

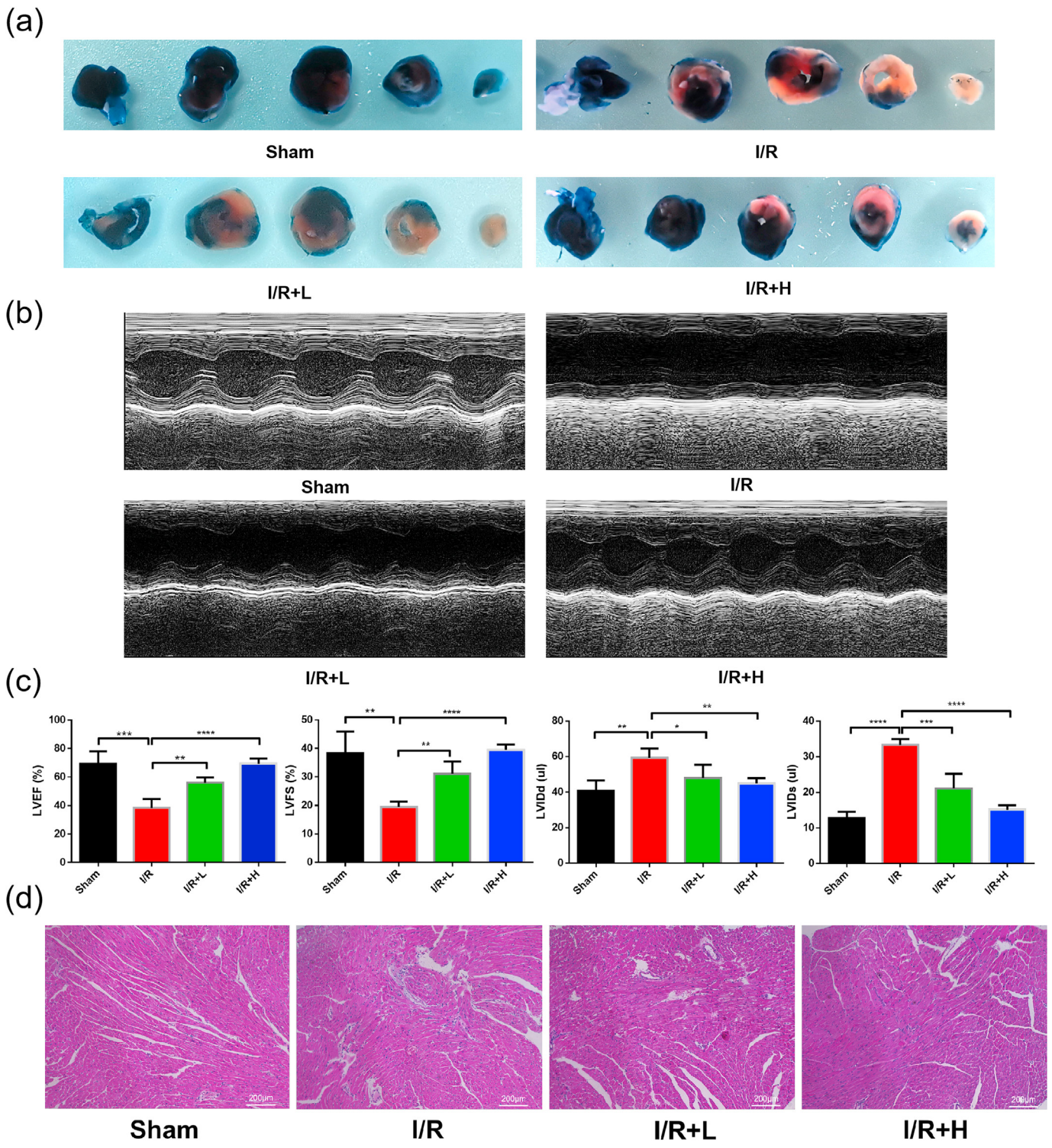

Fig. 7. (a) TTC-Evans blue staining shows myocardial hypoxic infarction (blue area: healthy tissue; red area: risk tissues; white area: infarct tissue). (b) Representative transthoracic M-mode echocardiograms from each group following either I/R or sham operation. (c) Quantification results of LVIDd, LVIDs, LVEF. and LVFS in each group (n = 5). (d) Representative images of HE staining, describe each group of myofibril edema circumstance in the acute phase of reperfusion. (Data are presented as the mean ± SD,n = 5, *P < 0.05, **P < 0.01, ***P < 0.001,****P < 0.0001, Bar = 200μm)

indicating that Nrf2/HO-1 signaling pathway was activated by Akt pathway in this experiment, and there was a positive correlation (Fig. 9b). Cell immunofluorescence also showed that $\mathbf{6M_1@C_{60}}$ could further promote Nrf2 expression and nuclear translocation under H_2O_2-induced oxidative stress (Fig. 9c). These data indicate that $\mathbf{6M_1@C_{60}}$ is involved in the regulation of Akt and Nrf2 signaling pathways.

2.8. Regulation of H_2O_2-induced apoptosis and inflammatory injury through Nrf2

Nrf2 signaling has also been shown to be modulated by a more complex regulatory network, including phosphoinositol 3-kinase (PI3K)/protein kinase B (Akt), protein kinase C, and mitogen-activated protein

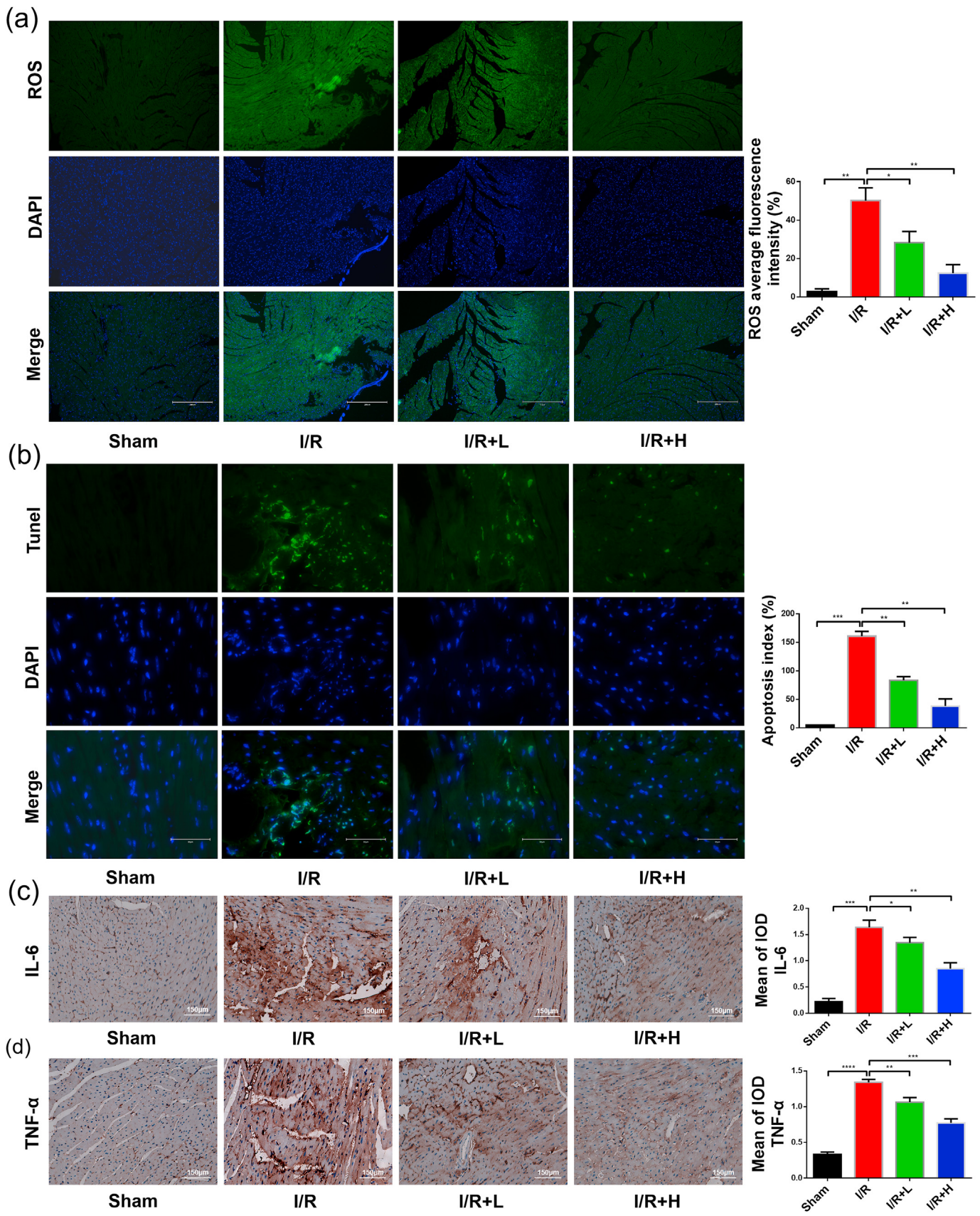

Fig. 8. (a) R.O.S. levels in the myocardium (n = 5). (b) Images of Tunel staining of the myocardium, green fluorescence represents apoptotic myocardial tissue. (c) Immunohistochemical staining of related inflammatory markers in the myocardium. (Data are presented as the mean ± SD,n = 5, *P < 0.05, **P < 0.01, ***P < 0.001,****P < 0.0001)

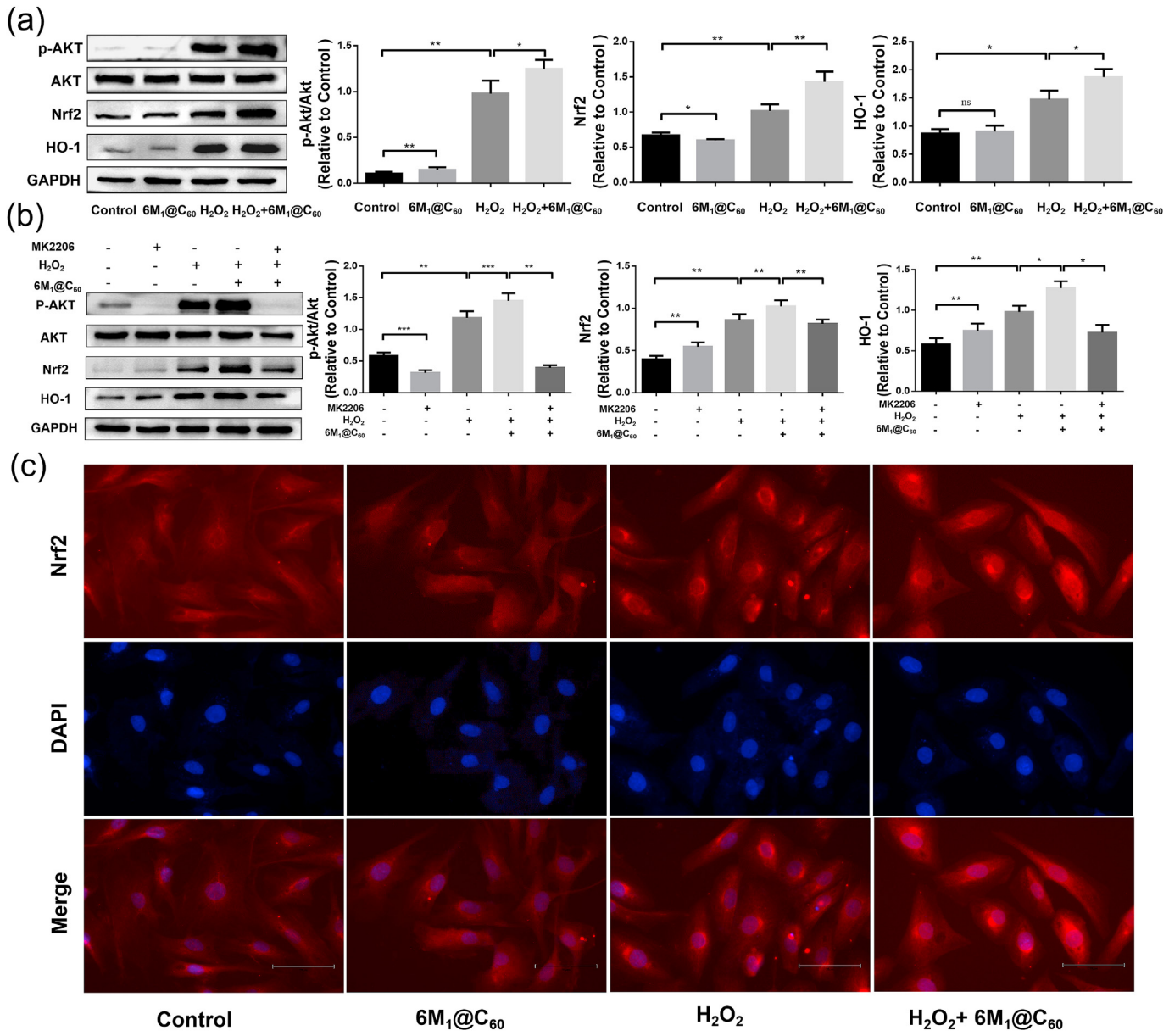

Fig. 9. (a) Effects of **$6M_1@C_{60}$** on the expression levels of Akt, p-Akt, Nrf2 and HO-1 proteins in cells. (b) The effect of **$6M_1@C_{60}$** on the expression levels of Akt, p-Akt, Nrf2 and HO-1 proteins in cells was observed of Akt blockade (MK2206). (c) Immunofluorescence analysis of Nrf2 localization. FMC84 cells were labeled with Nrf2 (red) and nuclei were stained with DAPI. (blue), Bar = 75 μm.(Data are presented as the mean ± S.D., n = 3, *P < 0.05, **P < 0.01, ***P < 0.001, NS means not significant)

kinase [55]. To further verify the role of Nrf2/HO-1 signaling in anti-apoptosis and inflammation and to verify whether Nrf2 and HO-1 are necessary factors for **$6M_1@C_{60}$** protective function, we pretreated cardiomyocytes with ML385, which is a highly specific Nrf2 inhibitor. Subsequently, we determined intracellular R.O.S. content by DCFH-DA and found that ML385 significantly reversed the scavenging effect of **$6M_1@C_{60}$** on H_2O_2-induced R.O.S. (Fig. 10a). W.B. data also showed that after inhibiting the effect of Nrf2, the inflammatory indicators such as IL-6, TNF-α and apoptosis indicator caspase3 did not reach the inhibitory effect (Fig. 10b). According to the obtained data, Nrf2 and HO-1 play a key role in **$6M_1@C_{60}$** regulated cytoprotection.

Oxidative stress has been widely implicated in numerous cardiovascular diseases, particularly myocardial infarction, myocardial ischemia-reperfusion injury, and atherosclerosis [56]. Reactive oxygen species (R.O.S.), such as H_2O_2, have been shown to induce cardiomyocyte apoptosis, which is recognized as a major contributor to chemoresistance in cardiovascular diseases [57,58]. The production of R.O.S. from sources such as the mitochondrial electron transport chain, fat oxidase, and catecholamine automatic oxidation causes a persistent oxidative damage that can lead to programmed cell death and the loss of functional cardiac cells [59]. Despite significant improvements in treatment strategies to reduce cardiovascular risk, the management of cardiovascular disease remains a challenging issue in developing countries.

Currently, a variety of therapies aim to balance oxidative stress with the disease, and large-scale clinical trials have demonstrated that using antioxidants (such as vitamin C, vitamin E and polyphenol) [60], cardiovascular drugs (such as statins, angiotensin-converting enzyme inhibitors, AT-1 receptor blockers, SGLT2 inhibitors and DPP-4 inhibitors) and immune modulators (such as cytokines of monoclonal antibody) shows a strong antioxidant effect [61]. Given the important role that antioxidants play in cardiovascular disease, new powerful antioxidants have been the focus of attention. Previous studies have shown that C_{60}

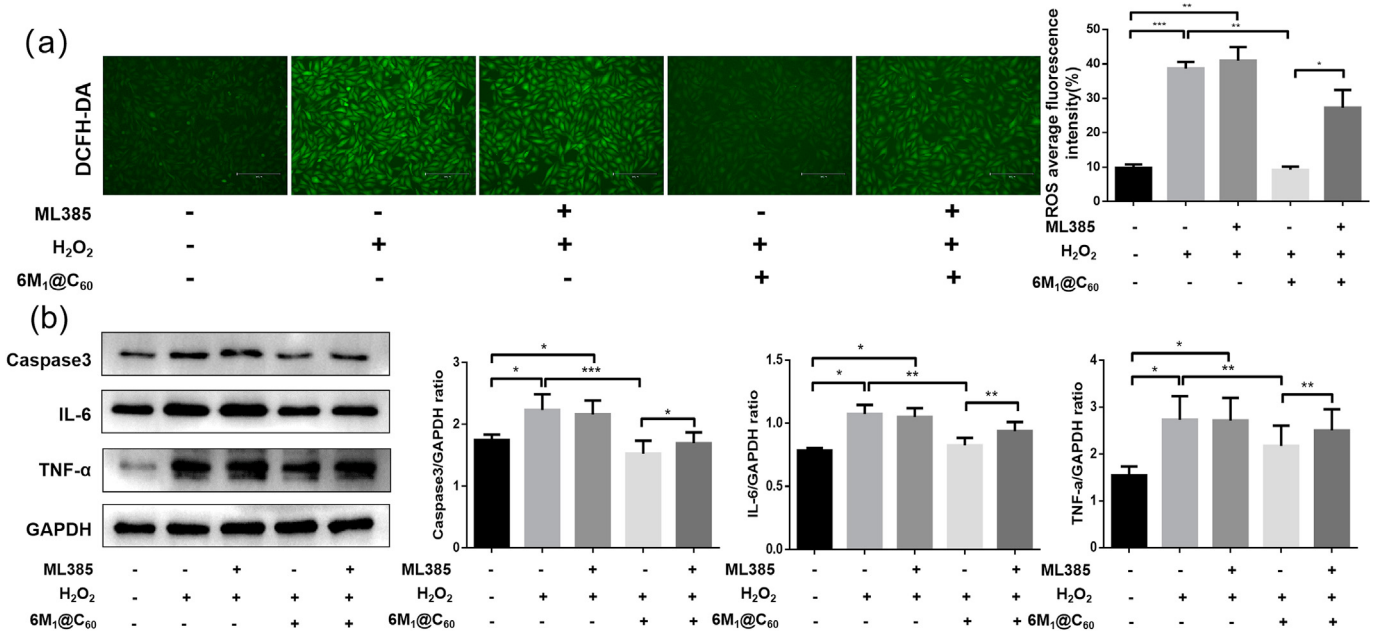

Fig. 10. (a) The fluorescence probe DCFH-DA was used to detect intracellular R.O.S. levels, Bar = 300 μm. (b) To observe the effect of **$6M_1@C_{60}$** on the protein expression levels of IL-6, TNF-α and Caspase3 in cells after Nrf2 was blocked by specific inhibitor ML385. (Data are presented as the mean ± SD,n = 3, *P < 0.05, **P < 0.01, ***P < 0.001).

not only shows great advantages in anti-oxidation but also plays a positive role in anti-apoptosis and anti-inflammatory [20,62,63]. Mei Ding et al. [64] found that fullerenol can improve cardiac function, reduce the inflammatory reaction, increase antioxidant function, and enhance the activity of Nrf2/HO-1 signaling pathway in myocardial cells. Through our research, we have also found that **$6M_1@C_{60}$** can prevent the deterioration of heart function caused by ischemia-reperfusion, and suppress apoptosis of cardiac myocytes, mitigating the progression of myocardial infarction. In addition, Borovic et al. [65] found that fullerols have potential protective effects on adriamycin pretreated porcine cardiomyocytes, mainly by reducing active oxygen species to improve cellular ultrastructures, such as reducing cavitation, pyknosis, interstitial edema and congestion. In order to further demonstrate the ability of **$6M_1@C_{60}$** to scavenge reactive oxygen species (R.O.S.), we also assessed the levels of R.O.S. in the ischemia-reperfusion region. The results showed that the involvement of **$6M_1@C_{60}$** effectively reduced the levels of R.O.S. in cardiac tissues, suppressed apoptosis of cardiac tissues, and alleviated the inflammatory response. In order to verify the feasibility of the novel water-soluble fullerenes constructed in this experiment, our experimental findings that H_2O_2 could reduce cell viability, increase intracellular R.O.S. levels, induce cell apoptosis and inflammatory response. By applying **$6M_1@C_{60}$**, we found that **$6M_1@C_{60}$** could significantly reduce the intracellular R.O.S. levels induced by H_2O_2, reverse the effects of H_2O_2 on cells, and improve cell viability. Using RT-qPCR and W.B. assays, we found that **$6M_1@C_{60}$** reduced the expression levels of apoptosis and inflammation-related proteins such as IL-6, TNF-α and Caspase3. In addition, we demonstrated that the realization of **$6M_1@C_{60}$** effect is related to the activation of Akt signaling pathway.

Akt plays an important role in the pathogenesis of cardiovascular diseases, and it is known that PI3K/Akt can regulate cell functions, such as cell migration, cell survival and other metabolic processes [66]. For example, the activation of PI3K/Akt signaling pathway can effectively inhibit the apoptosis of cardiomyocytes and improve cardiac function in rats with acute myocardial infarction. Akt also functions as a survival kinase by influencing nuclear factor-κB (NF-κB) and glycogen synthase kinase (GSK-3β) by phosphorylating many apoptotic regulatory molecules, such as forkhead transcription factor, caspase 9, and IκB kinase (IKKα) [67,68]. In this study, we found that intracellular Akt phosphorylation increased in response to H_2O_2-induced oxidative stress, triggering cellular defense mechanisms. The involvement of **$6M_1@C_{60}$** further increased the phosphorylation of Akt and further activated the Akt signaling pathway to play an anti-apoptotic and inflammatory role. In order to further explore the specific regulatory mechanism of Akt, we selected the classical antioxidant pathway Nrf2/HO-1. Previous studies have also shown that activation of Nrf2 inhibits left ventricular remodeling and heart failure due to ventricular remodeling [69,70]. Cheng et al. [71] also found that Nrf2 deficiency in mice increased ox-LDL-induced foam cell formation, suggesting that this gene has an atheroprotective role. We found that phosphorylation of Akt increased the expression of Nrf2/HO-1, and the production of Nrf2 and HO-1 attenuated the apoptosis and inflammatory response of cardiomyocytes. In our experiment, the anti-apoptotic and anti-inflammatory effects of **$6M_1@C_{60}$** were significantly inhibited after the use of Nrf2 specific inhibitors. Therefore, it shows that Nrf2/HO-1 plays a certain role in coping with H_2O_2-induced oxidative stress. In brief, we have discovered that **$6M_1@C_{60}$** possesses the potential to safeguard mouse cardiomyocytes against R.O.S. injury by exerting anti-apoptotic and antioxidant effects. Additionally, it may ameliorate the decline in cardiac function attributable to ischemia-reperfusion, attenuate myofibril edema, decrease myocardial R.O.S. levels, suppress cardiomyocyte apoptosis, and mitigate inflammatory responses. The underlying mechanism of action appears to involve the Akt and Nrf2/HO-1 signaling pathways. All these positive results are derived from the innovation of the materials. The increased solubility of the C_{60} in water through supramolecular self-assembly is a necessary premise for the development of this project. The suitable cavity size of the supramolecular cage makes it a perfect capsule for C_{60}. The significant improvement of the water solubility of the C_{60} complex does not cause any change in the structure of the C_{60} parent. Thus, excellent antioxidant activity is maintained.

3. Conclusions

C_{60} can scavenge oxygen-free radicals, but its poor water solubility limits its clinical application. The purpose of this study is to develop a water-soluble cage that could encapsulate C_{60} molecule to improve its

water solubility and explore its protective effect on oxidative stress-induced myocardial injury. A water-soluble cube-like supramolecular cage was constructed by an engagement of six molecules through a hydrophobic effect in the water. The obtained cage could perfectly encapsulate one C_{60} molecule inside of the cavity and significantly improve the water-solubility of the C_{60} without changing the original structure of C_{60}. Furthermore, our investigations also revealed that C_{60} exhibited the potential to reverse hydrogen peroxide-induced myocardial injury under appropriate time and dose conditions, promoting cell viability, markedly reducing intracellular R.O.S. levels, and mitigating apoptosis and inflammation. Moreover, it improved the deterioration of cardiac function in mice affected by myocardial ischemia-reperfusion injury, decreased the R.O.S. levels in myocardial tissue, inhibited myocardial apoptosis, and lowered myocardial inflammatory reactions. We delved deeper into the related signal pathway and verified its role by utilizing corresponding inhibitors. The results showed that C_{60} protected cells by activating the Akt and Nrf2/HO-1 pathway, and this protective effect was blocked by Akt inhibitor (MK2206) and Nrf2 inhibitor (ML385). The present study provides a new guideline for constructing water-soluble C_{60} and verifies the important role of C_{60} in preventing oxidative stress-related cardiovascular disease injury.

Credit author statement

Guanzhao Zhang: Biological experiments. Hui Fang: Synthesis of the cage and the cage/C60 complex. Shuting Chang: Biological experiments. Renzeng Chen: Single crystal of the cage. Lanlan Li: Biological experiments. Danbo Wan: Simulation of the cage/C60 complex. Yamei Liu: Synthesis of the cage. Ruyi Sun: Guide some synthesis of the cage. Yingjie Zhao: Conceptualization and supervision of the chemical part (cage and C60). Bo Li: Conceptualization and supervision of the biological part.

Declaration of competing interest

The authors declare that they have no known competing financial interests or personal relationships that could have appeared to influence the work reported in this paper.

Data availability

Data will be made available on request.

Acknowledgements

The work was supported by the National Natural Science Foundation of China (81370325, 31202117) and Natural Science Foundation of Shandong Province (ZR2020MH025, ZR2020ZD38).

Appendix A. Supplementary data

Supplementary data to this article can be found online at https://doi.org/10.1016/j.mtbio.2023.100693.

References

[1] R.G. Jung, P. Di Santo, R. Mathew, O. Abdel-Razek, S. Parlow, T. Simard, J.A. Marbach, T. Gillmore, B. Mao, J. Bernick, P. Theriault-Lauzier, A. Fu, L. Lau, P. Motazedian, J.J. Russo, M. Labinaz, B. Hibbert, Implications of myocardial infarction on management and outcome in cardiogenic shock, J. Am. Heart Assoc. 10 (21) (2021), e021570, https://doi.org/10.1161/jaha.121.021570.

[2] K. Jinawong, N. Apaijai, N. Chattipakorn, S.C. Chattipakorn, Cognitive impairment in myocardial infarction and heart failure, Acta Physiol. 232 (1) (2021), e13642, https://doi.org/10.1111/apha.13642.

[3] S. Frantz, M.J. Hundertmark, J. Schulz-Menger, F.M. Bengel, J. Bauersachs, Left ventricular remodelling post-myocardial infarction: pathophysiology, imaging, and novel therapies, Eur. Heart J. 43 (27) (2022) 2549–2561, https://doi.org/10.1093/eurheartj/ehac223.

[4] S.B. Ong, S. Hernández-Reséndiz, G.E. Crespo-Avilan, R.T. Mukhametshina, X.Y. Kwek, H.A. Cabrera-Fuentes, D.J. Hausenloy, Inflammation following acute myocardial infarction: multiple players, dynamic roles, and novel therapeutic opportunities, Pharmacol. Ther. 186 (2018) 73–87, https://doi.org/10.1016/j.pharmthera.2018.01.001.

[5] G. Heusch, B.J. Gersh, The pathophysiology of acute myocardial infarction and strategies of protection beyond reperfusion: a continual challenge, Eur. Heart J. 38 (11) (2017) 774–784, https://doi.org/10.1093/eurheartj/ehw224.

[6] M. Dambrova, C.J. Zuurbier, V. Borutaite, E. Liepinsh, M. Makrecka-Kuka, Energy substrate metabolism and mitochondrial oxidative stress in cardiac ischemia/reperfusion injury, Free Radical Biol. Med. 165 (2021) 24–37, https://doi.org/10.1016/j.freeradbiomed.2021.01.036.

[7] M.Y. Wu, G.T. Yiang, W.T. Liao, A.P. Tsai, Y.L. Cheng, P.W. Cheng, C.Y. Li, C.J. Li, Current mechanistic concepts in ischemia and reperfusion injury, cellular physiology and biochemistry, international journal of experimental cellular physiology, biochemistry, and pharmacology 46 (4) (2018) 1650–1667, https://doi.org/10.1159/000489241.

[8] N. García, C. Zazueta, L. Aguilera-Aguirre, Oxidative Stress and Inflammation in Cardiovascular Disease, Oxidative Medicine and Cellular Longevity 2017, 2017, 5853238, https://doi.org/10.1155/2017/5853238.

[9] N. Zarkovic, Roles and functions of R.O.S. And R.N.S. In cellular physiology and pathology, Cells 9 (3) (2020), https://doi.org/10.3390/cells9030767.

[10] N. Sinha, P.K. Dabla, Oxidative stress and antioxidants in hypertension-a current review, Curr. Hypertens. Rev. 11 (2) (2015) 132–142, https://doi.org/10.2174/1573402111666150529130922.

[11] X. Li, N. Xiang, Z. Wang, Ginsenoside Rg2 attenuates myocardial fibrosis and improves cardiac function after myocardial infarction via A.K.T. signaling pathway, Biosc. Biotech. Biochem. 84 (11) (2020) 2199–2206, https://doi.org/10.1080/09168451.2020.1793292.

[12] Y. Zhang, P. Murugesan, K. Huang, H. Cai, NADPH oxidases and oxidase crosstalk in cardiovascular diseases: novel therapeutic targets, Nat. Rev. Cardiol. 17 (3) (2020) 170–194, https://doi.org/10.1038/s41569-019-0260-8.

[13] M. Hori, K. Nishida, Oxidative stress and left ventricular remodelling after myocardial infarction, Cardiovasc. Res. 81 (3) (2009) 457–464, https://doi.org/10.1093/cvr/cvn335.

[14] A. Belló-Klein, N. Khaper, S. Llesuy, D.V. Vassallo, C.J.O.M. Pantos, C. Longevity, Oxidative Stress and Antioxidant Strategies in Cardiovascular Disease, 2014, 2014, 678741. https://doi.org/10.1155/2014/678741.

[15] E.G. Rosenbaugh, K.K. Savalia, D.S. Manickam, M.C. Zimmerman, Antioxidant-based therapies for angiotensin II-associated cardiovascular diseases, Am. J. Physiol. Regul. Integr. Comp. Physiol. 304 (11) (2013) R917–R928, https://doi.org/10.1152/ajpregu.00395.2012.

[16] K.J. Bubb, G.R. Drummond, G.A. Figtree, New opportunities for targeting redox dysregulation in cardiovascular disease, Cardiovasc. Res. 116 (3) (2020) 532–544, https://doi.org/10.1093/cvr/cvz183.

[17] P.J. Krusic, E. Wasserman, P.N. Keizer, J.R. Morton, K.F. Preston, Radical reactions of c60, Science (New York, N.Y.) 254 (5035) (1991) 1183–1185, https://doi.org/10.1126/science.254.5035.1183.

[18] J.-J. Yin, F. Lao, P.P. Fu, W.G. Wamer, Y. Zhao, P.C. Wang, Y. Qiu, B. Sun, G. Xing, J. Dong, X.-J. Liang, C. Chen, The scavenging of reactive oxygen species and the potential for cell protection by functionalized fullerene materials, Biomaterials 30 (4) (2009) 611–621, https://doi.org/10.1016/j.biomaterials.2008.09.061.

[19] L. Xiao, H. Takada, X. Gan, N. Miwa, The water-soluble fullerene derivative "Radical Sponge" exerts cytoprotective action against UVA irradiation but not visible-light-catalyzed cytotoxicity in human skin keratinocytes, Bioorg. Med. Chem. Lett 16 (6) (2006) 1590–1595, https://doi.org/10.1016/j.bmcl.2005.12.011.

[20] V.A. Chistyakov, Y.O. Smirnova, E.V. Prazdnova, A.V. Soldatov, Possible mechanisms of fullerene C_{60} antioxidant action, BioMed Res. Int. 2013 (2013), 821498, https://doi.org/10.1155/2013/821498.

[21] D.Y. Lyon, L.K. Adams, J.C. Falkner, P.J. Alvarezt, Antibacterial activity of fullerene water suspensions: effects of preparation method and particle size, Environ. Sci. Technol. 40 (14) (2006) 4360–4366, https://doi.org/10.1021/es0603655.

[22] S. Dostalova, A. Moulick, V. Milosavljevic, R. Guran, M. Kominkova, K. Cihalova, Z. Heger, L. Blazkova, P. Kopel, D. Hynek, M. Vaculovicova, V. Adam, R. Kizek, Antiviral activity of fullerene C60 nanocrystals modified with derivatives of anionic antimicrobial peptide maximin H5, Monatshefte für Chemie - Chemical Monthly 147 (5) (2016) 905–918, https://doi.org/10.1007/s00706-016-1675-0.

[23] M. Kumar, K. Raza, C60-fullerenes as drug delivery carriers for anticancer agents: promises and hurdles, Pharm. Nanotechnol. 5 (3) (2017) 169–179, https://doi.org/10.2174/2211738505666170301142232.

[24] M. Guan, Y. Zhou, S. Liu, D. Chen, J. Ge, R. Deng, X. Li, T. Yu, H. Xu, D. Sun, J. Zhao, T. Zou, C. Wang, C. Shu, Photo-triggered gadofullerene: enhanced cancer therapy by combining tumor vascular disruption and stimulation of anti-tumor immune responses, Biomaterials 213 (2019), 119218, https://doi.org/10.1016/j.biomaterials.2019.05.029.

[25] R. Bakry, R.M. Vallant, M. Najam-ul-Haq, M. Rainer, Z. Szabo, C.W. Huck, G.K. Bonn, Medicinal applications of fullerenes, Int. J. Nanomed. 2 (4) (2007) 639–649.

[26] S. Goodarzi, T. Da Ros, J. Conde, F. Sefat, M. Mozafari, Fullerene: biomedical engineers get to revisit an old friend, Mater. Today 20 (8) (2017) 460–480, https://doi.org/10.1016/j.mattod.2017.03.017.

[27] L.M. Skivka, S.V. Prylutska, M.P. Rudyk, N.M. Khranovska, I.V. Opeida, V.V. Hurmach, Y.I. Prylutskyy, L.F. Sukhodub, U. Ritter, C(60) fullerene and its nanocomplexes with anticancer drugs modulate circulating phagocyte functions and dramatically increase R.O.S. generation in transformed monocytes, Cancer nanotechnology 9 (1) (2018) 8, https://doi.org/10.1186/s12645-017-0034-0.

[28] J. Li, M. Chen, S. Hou, L. Zhao, T. Zhang, A. Jiang, H. Li, J.J.C.A.I.J.S.b.t.A.C.S. Hao, Porous Organic-Inorganic Hybrids with Nonlinear Optical Properties from

Fullerenols-Metal Complexation, 2022, p. 191, https://doi.org/10.1016/j.carbon.2022.02.032.
[29] E. Nakamura, H. Isobe, Functionalized fullerenes in water. The first 10 years of their chemistry, biology, and nanoscience, Acc. Chem. Res. 36 (11) (2003) 807–815, https://doi.org/10.1021/ar030027y.
[30] C.M. Sayes, J.D. Fortner, W. Guo, D. Lyon, A.M. Boyd, K.D. Ausman, Y.J. Tao, B. Sitharaman, L.J. Wilson, J.B.J.N.L. Hughes, The Differential Cytotoxicity of Water-Soluble Fullerenes 4 (10) (2004) 1881–1887, https://doi.org/10.1021/nl0489586.
[31] J. Li, M. Chen, S. Zhou, H. Li, J. Hao, Self-assembly of fullerene C(60)-based amphiphiles in solutions, Chem. Soc. Rev. 51 (8) (2022) 3226–3242, https://doi.org/10.1039/d1cs00958c.
[32] S.P. Wang, W. Lin, X. Wang, T.Y. Cen, H. Xie, J. Huang, B.Y. Zhu, Z. Zhang, A. Song, J. Hao, J. Wu, S. Li, Controllable hierarchical self-assembly of porphyrin-derived supra-amphiphiles, Nat. Commun. 10 (1) (2019) 1399, https://doi.org/10.1038/s41467-019-09363-y.
[33] S. Hiraoka, K. Harano, M. Shiro, M. Shionoya, A self-assembled organic capsule formed from the union of six hexagram-shaped amphiphile molecules, J. Am. Chem. Soc. 130 (44) (2008) 14368–14369, https://doi.org/10.1021/ja804885k.
[34] X. Zhang, C. Wang, Supramolecular amphiphiles, Chem. Soc. Rev. 40 (1) (2011) 94–101, https://doi.org/10.1039/b919678c.
[35] G. Yu, K. Jie, F. Huang, Supramolecular amphiphiles based on host-guest molecular recognition motifs, Chem. Rev. 115 (15) (2015) 7240–7303, https://doi.org/10.1021/cr5005315.
[36] S. Chen, R. Costil, F.K. Leung, B.L. Feringa, Self-assembly of photoresponsive molecular amphiphiles in aqueous media, Angew. Chem. 60 (21) (2021) 11604–11627, https://doi.org/10.1002/anie.202007693.
[37] B. Hu, N. Song, Y. Cao, M. Li, X. Liu, Z. Zhou, L. Shi, Z. Yu, Noncanonical amino acids for hypoxia-responsive peptide self-assembly and fluorescence, J. Am. Chem. Soc. 143 (34) (2021) 13854–13864, https://doi.org/10.1021/jacs.1c06435.
[38] Y. Li, J. Dong, W. Gong, X. Tang, Y. Liu, Y. Cui, Y. Liu, Artificial biomolecular channels: enantioselective transmembrane transport of amino acids mediated by homochiral zirconium metal-organic cages, J. Am. Chem. Soc. 143 (49) (2021) 20939–20951, https://doi.org/10.1021/jacs.1c09992.
[39] T. Nishimura, K. Akiyoshi, Artificial molecular chaperone systems for proteins, nucleic acids, and synthetic molecules, Bioconjugate Chem. 31 (5) (2020) 1259–1267, https://doi.org/10.1021/acs.bioconjchem.0c00133.
[40] L. Tapia, I. Alfonso, J. Solà, Molecular cages for biological applications, Org. Biomol. Chem. 19 (44) (2021) 9527–9540, https://doi.org/10.1039/d1ob01737c.
[41] G. Yu, T.Y. Cen, Z. He, S.P. Wang, Z. Wang, X.W. Ying, S. Li, O. Jacobson, S. Wang, L. Wang, L.S. Lin, R. Tian, Z. Zhou, Q. Ni, X. Li, X. Chen, Porphyrin nanocage-embedded single-molecular nanoparticles for cancer nanotheranostics, Angew. Chem. 58 (26) (2019) 8799–8803, https://doi.org/10.1002/anie.201903277.
[42] H. Takezawa, R. Tabuchi, H. Sunohara, M. Fujita, Confinement of water-soluble cationic substrates in a cationic molecular cage by capping the portals with tripodal anions, J. Am. Chem. Soc. 142 (42) (2020) 17919–17922, https://doi.org/10.1021/jacs.0c08835.
[43] G. Montà-González, F. Sancenón, R. Martínez-Máñez, V. Martí-Centelles, Purely covalent molecular cages and containers for guest encapsulation, Chem. Rev. 122 (16) (2022) 13636–13708, https://doi.org/10.1021/acs.chemrev.2c00198.
[44] D. Wang, L. Zhang, Y. Zhao, Template-free synthesis of an interlocked covalent organic molecular cage, J. Org. Chem. 87 (5) (2022) 2767–2772, https://doi.org/10.1021/acs.joc.1c02688.
[45] C. Tan, D. Chu, X. Tang, Y. Liu, W. Xuan, Y. Cui, Supramolecular coordination cages for asymmetric catalysis, Chemistry 25 (3) (2019) 662–672, https://doi.org/10.1002/chem.201802817.
[46] K. Yazaki, M. Akita, S. Prusty, D.K. Chand, T. Kikuchi, H. Sato, M. Yoshizawa, Polyaromatic molecular peanuts, Nat. Commun. 8 (2017), 15914, https://doi.org/10.1038/ncomms15914.
[47] E.G. Percástegui, T.K. Ronson, J.R. Nitschke, Design and applications of water-soluble coordination cages, Chem. Rev. 120 (24) (2020) 13480–13544, https://doi.org/10.1021/acs.chemrev.0c00672.
[48] J. Padmanabhan, T.R. Kyriakides, Nanomaterials, inflammation, and tissue engineering, Wiley interdisciplinary reviews, Nanomedicine and nanobiotechnology 7 (3) (2015) 355–370, https://doi.org/10.1002/wnan.1320.
[49] H. Su, Y. Wang, Y. Gu, L. Bowman, J. Zhao, M. Ding, Potential applications and human biosafety of nanomaterials used in nanomedicine, J. Appl. Toxicol. : JAT (J. Appl. Toxicol.) 38 (1) (2018) 3–24, https://doi.org/10.1002/jat.3476.
[50] X. Zhu, M. Sollogoub, Y. Zhang, Biological applications of hydrophilic C60 derivatives (hC60s)- a structural perspective, Eur. J. Med. Chem. 115 (2016) 438–452, https://doi.org/10.1016/j.ejmech.2016.03.024.
[51] T.R. Welberry, in: J.T. Atwood, J.W. Steed (Eds.), Encyclopedia of Supramolecular Chemistry, CRC Press, Boca Raton, FL, 2004, pp. 457–466.
[52] K. Rissanen, in: J.T. Atwood, J.W. Steed (Eds.), Encyclopedia of Supramolecular Chemistry, CRC Press, Boca Raton, FL, 2004, pp. 1586–1591.
[53] R. Kang, R. Li, P. Dai, Z. Li, Y. Li, C. Li, Deoxynivalenol induced apoptosis and inflammation of IPEC-J2 cells by promoting R.O.S. production, Environ. Pollut. 251 (2019) 689–698, https://doi.org/10.1016/j.envpol.2019.05.026.
[54] N. Katila, S. Bhurtel, P.H. Park, D.Y. Choi, Metformin attenuates rotenone-induced oxidative stress and mitochondrial damage via the A.K.T./Nrf2 pathway, Neurochem. Int. 148 (2021), 105120, https://doi.org/10.1016/j.neuint.2021.105120.
[55] C. Yu, J.H. Xiao, The keap1-nrf2 system: a mediator between oxidative stress and aging, Oxid. Med. Cell. Longev. 2021 (2021), 6635460, https://doi.org/10.1155/2021/6635460.
[56] S.S. Singh, P.M. Kang, Mechanisms and inhibitors of apoptosis in cardiovascular diseases, Curr. Pharmaceut. Des. 17 (18) (2011) 1783–1793, https://doi.org/10.2174/138161211796390994.
[57] J. Xie, X. Zhou, X. Hu, H. Jiang, H2O2 evokes injury of cardiomyocytes through upregulating HMGB1, Hellenic journal of cardiology, H.J.C. = Hellenike kardiologike epitheorese 55 (2) (2014) 101–106.
[58] P.M. Kang, S. Izumo, Apoptosis in heart: basic mechanisms and implications in cardiovascular diseases, Trends Mol. Med. 9 (4) (2003) 177–182, https://doi.org/10.1016/s1471-4914(03)00025-x.
[59] J. Dan Dunn, L.A. Alvarez, X. Zhang, T. Soldati, Reactive oxygen species and mitochondria: a nexus of cellular homeostasis, Redox Biol. 6 (2015) 472–485, https://doi.org/10.1016/j.redox.2015.09.005.
[60] H.N. Siti, Y. Kamisah, J. Kamsiah, The role of oxidative stress, antioxidants and vascular inflammation in cardiovascular disease (a review), Vasc. Pharmacol. 71 (2015) 40–56, https://doi.org/10.1016/j.vph.2015.03.005.
[61] U. Förstermann, Oxidative stress in vascular disease: causes, defense mechanisms and potential therapies, Nature clinical practice, Cardiovasc. Med. 5 (6) (2008) 338–349, https://doi.org/10.1038/ncpcardio1211.
[62] N. Shershakova, E. Baraboshkina, S. Andreev, D. Purgina, I. Struchkova, O. Kamyshnikov, A. Nikonova, M. Khaitov, Anti-inflammatory effect of fullerene C60 in a mice model of atopic dermatitis, J. Nanobiotechnol. 14 (2016) 8, https://doi.org/10.1186/s12951-016-0159-z.
[63] Z. Hu, W. Guan, W. Wang, Z. Zhu, Y. Wang, Folacin C60 derivative exerts a protective activity against oxidative stress-induced apoptosis in rat pheochromocytoma cells, Bioorg. Med. Chem. Lett 20 (14) (2010) 4159–4162, https://doi.org/10.1016/j.bmcl.2010.05.062.
[64] M. Ding, M. Li, E.M. Zhang, H.L. Yang, FULLEROL alleviates myocardial ischemia-reperfusion injury by reducing inflammation and oxidative stress in cardiomyocytes via activating the Nrf2/HO-1 signaling pathway, Eur. Rev. Med. Pharmacol. Sci. 24 (18) (2020) 9665–9674, https://doi.org/10.26355/eurrev_202009_23056.
[65] M.L. Borović, I. Ičević, Z. Kanački, D. Žikić, M. Seke, R. Injac, A. Djordjević, Effects of fullerenol C60(OH)24 nanoparticles on a single-dose doxorubicin-induced cardiotoxicity in pigs: an ultrastructural study, Ultrastruct. Pathol. 38 (2) (2014) 150–163, https://doi.org/10.3109/01913123.2013.822045.
[66] A. Eisenreich, U. Rauch, PI3K inhibitors in cardiovascular disease, Cardiovascular therapeutics 29 (1) (2011) 29–36, https://doi.org/10.1111/j.1755-5922.2010.00206.x.
[67] F. Chen, Z.Q. Chen, H. Wang, J.J. Zhu, Puerarin pretreatment inhibits myocardial apoptosis and improves cardiac function in rats after acute myocardial infarction through the PI3K/Akt signaling pathway, Adv. Clin. Exp. Med. : official organ Wroclaw Medical University 30 (3) (2021) 255–261, https://doi.org/10.17219/acem/131754.
[68] W. Qin, L. Cao, I.Y. Massey, Role of PI3K/Akt signaling pathway in cardiac fibrosis, Mol. Cell. Biochem. 476 (11) (2021) 4045–4059, https://doi.org/10.1007/s11010-021-04219-w.
[69] R. Howden, Nrf2 and Cardiovascular Defense, Oxidative Medicine and Cellular Longevity 2013, 2013, 104308, https://doi.org/10.1155/2013/104308.
[70] R.M. da Costa, D. Rodrigues, C.A. Pereira, J.F. Silva, J.V. Alves, N.S. Lobato, R.C. Tostes, Nrf2 as a potential mediator of cardiovascular risk in metabolic diseases, Front. Pharmacol. 10 (2019) 382, https://doi.org/10.3389/fphar.2019.00382.
[71] S. Zhou, W. Sun, Z. Zhang, Y. Zheng, The role of Nrf2-mediated pathway in cardiac remodeling and heart failure, Oxid. Med. Cell. Longev. 2014 (2014), 260429, https://doi.org/10.1155/2014/260429.